

# LEAF SEGMENTATION OF ROSETTE PLANTS USING ROUGH K-MEANS IN CIELAB COLOR SPACE

Arunita Das \*

Dept. of Computer Science and Application  
Midnapore College (Autonomous)  
Paschim Medinipur, West Bengal, India  
arunita17@gmail.com

Daipayan Ghosal

Dept. of Computer Science and Application  
Midnapore College (Autonomous)  
Paschim Medinipur, West Bengal, India  
daipayan.ghosal@gmail.com

Krishna Gopal Dhal †

Dept. of Computer Science and Application  
Midnapore College (Autonomous)  
Paschim Medinipur, West Bengal, India  
krishnagopal.dhal@midnaporecollege.ac.in

## ABSTRACT

Segmentation of Plant Images plays an important role in modern agriculture where it can provide accurate analysis of a plant's growth and possible anomalies. In this paper, rough set based partitionial clustering technique called Rough K-Means has been utilized in CIELab color space for the proper leaf segmentation of rosette plants. The efficacy of the proposed technique have been analysed by comparing it with the results of traditional K-Means and Fuzzy C-Means clustering algorithms. The visual and numerical results reveal that the RKM in CIELab provides the nearest result to the ideal ground truth, hence the most efficient one.

**Keywords** image segmentation, color space, rough set, partitionial clustering

## 1 Introduction

Leaf check and leaf region (i.e., plant area) are the key plant phenotyping qualities used to examine the plant development and advancement [19] [25] [28], blossoming time [13], and yield potential. The leaf include can be tended to in different manners from the AI viewpoint [1]. One such route is to check the number of leaves from fragmented plant area. Several image segmentation techniques are reported in literature for leaf segmentation. For example, Maximal Similarity-based Region Merging (MSRM) [18] is an intuitive segmentation approach which utilizes a region merging framework to meld super-pixel division. gPb-owt-ucm [2] is another segmentation method which is dependent on spectral clustering and contour detection. The IPK technique [20] utilized 3D histogram of  $L^*a^*b^*$  tone space of the plant images for regulated segmentation of closer view/foundation.

Vukadinovic and Polder employed neural networks combined with watershed for leaves segmentation [24]. A col-

lation study among several leaf segmentation algorithms had been presented in [27]. Well-known clustering techniques like KM, FCM, Self-organizing Map (SOM), and Particle Swarm Optimization (PSO) are also applied for leaf segmentation in [11] and SOM outperforms other tested methods visually and numerically. Other than the above techniques, deep learning is also utilized for the leaf segmentation [15]. However, deep learning needs large dataset in order to produce good results.

Therefore, it can be seen from the above discussion that different clustering strategies provide promising segmentation results. Although classical KM, FCM, SOM, and PSO are utilized for leaf segmentation, but rough set based K-Means (RKM) clustering did not used in this area according to the knowledge of the authors. Rough k-means is developed by Lingras et al. [16] and a refined version is proposed by Peters [21] and it shows the performance in image clustering domain as a similarity based clustering model like KM and FCM [14] [10] [12] [22]. RKM has been efficiently applied for the proper segmentation of tumor region from brain MRI images [14] [10], White blood cell segmentation [12], and satellite image segmentation [22]. As a consequence, the main contribution of the paper is the utilization of RKM in CIELab and its application for leaf segmentation. The proposed methodology which is represented in Figure 1 has been compared with classical KM and FCM. Experimental results show the supremacy of the proposed approach over other tested techniques.

The rest of the paper is organized as follows: Section 2 discusses the proposed methodology. Section 3 describes the experimental results and the paper is concluded in section 4.

## 2 Proposed Methodology

Clustering is a procedure of consortium a bunch of data into clusters that have superior intra-cluster and inferior inter-cluster resemblance among clusters. Two rudimentary types of image clustering practices are hard clustering and soft clustering. In hard clustering, one pixel can be the adherent of only one cluster and the proper exam-

\*First Author

†Corresponding Author



ple of this is K-means [5] [9] [7]. On the contrary of the previous one, soft clustering uses a miniscule membership unlike hard clustering which makes it more practicable for real world usages. One pixel can be the fragment of several clusters with some degree of belongingness which is described by the fractional membership. Fuzzy C-means is a specimen of this mechanism which had been projected by Bezdek [3] [6]. FCM is better than hard clustering technique like K-means because it has the more ability to handle the ambiguity of gray levels. In some cases, the fuzzy degree of membership may be too descriptive for interpreting clustering results. Therefore, researchers have applied rough set theory into k-means and developed rough k-means [16] [21] clustering algorithm which manages these equidistant data objects or overlapping clusters using upper and lower approximations of each cluster. Rough set-based clustering provides a solution that is less restrictive than conventional clustering and less descriptive (specific) than fuzzy clustering. In this study, Rough K-Means has been utilized to segment the leaf images. Due to non-uniform illumination of regions, the segmentation algorithm's performance is influenced by the color spaces used. According to the literature, perceptually uniform color spaces such as  $L^*a^*b^*$  or  $L^*u^*v^*$  achieve much better segmentation results than non-uniform color spaces such as RGB [23], which was developed for better color representation. As a first stage in our approach, we used MATLAB to transform all RGB images to CIE  $L^*a^*b^*$  color space, which yielded three components:  $L^*$ ,  $a^*$ , and  $b^*$ . " $L^*$ " denotes lightness, while " $a^*$ " and " $b^*$ " denote colors, with " $a^*$ " denoting red-green and " $b^*$ " denoting blue-yellow, respectively. The flowchart of the proposed work is presented in Figure 1 The brief mathematical implementation of RKM is described in section 2.1.

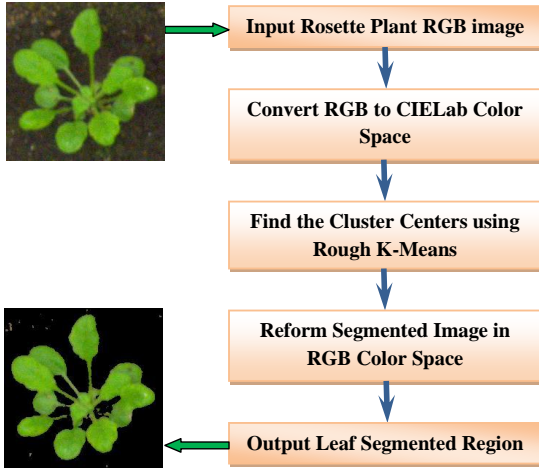


Figure 1: Flowchart of the Proposed Methodology

## 2.1 Rough K-Means (RKM)

Suppose, a hypothetical clustering scheme is defined as Eq. (1) which partitions  $U$  depending on the equivalence relation  $P$ . Again, assume that it may not be possible to accurately describe the sets  $C_i, 1 \leq i \leq k$  due to inadequate knowledge in the partition. But it is possible to

define each set  $C_i \in U/P$  using its lower approximation  $\underline{A}(C)$  and upper approximation  $\bar{A}(C)$ .

$$U/P = \{C_1, C_2, \dots, C_k\} \quad (1)$$

Let,  $v$  and  $c_i$  are the vector representation of the data object and cluster  $C_i$  respectively. Upper and lower approximations of only a few subsets of  $U$  have been considered. Hence, it is not possible to verify all the properties of the rough sets [16] [21]. However, the upper and lower estimates of  $C_i \in U/P$  are obligatory to follow some of the basic rough set properties which are as follows:

P1: A data entity  $v$  can be a participant of at most one lower approximation  $\underline{A}(c_i)$ .

P2: If a data object  $v$  is the portion of the lower approximation  $\underline{A}(c_i)$ , then it is also portion of the upper approximation  $\bar{A}(C)$  i.e.,  $v \in \underline{A}(c_i) \implies v \in \bar{A}(c_i)$ .

P3: If a data article  $v$  does not belong to any lower approximation  $\underline{A}(c_i)$  then it belongs to two or more upper approximations  $\bar{A}(c_i)$ .

In rough k-means, the lower and upper approximations of the clusters have been computed by the following rules: Let  $v$  be a data object and  $d(v, z_i)$  be the distance between  $v$  and  $z_i$  which is the centroid of cluster  $c_i$ .

Let  $d(v, z_i) = \min_{(1 \leq j \leq k)} d(v, z_j)$

$$T = \left\{ j : \frac{d(v, z_i)}{d(v, z_j)} \leq th \text{ and } i \neq j \right\} \quad (2)$$

Where,  $th$  is the threshold value specified by the user. In order to classify a data object to the correct approximation(s), the following classification criteria are being used:

**R1:** If the set,  $T$  is not an empty set, then the data object is classified as upper approximation of both cluster  $i$  and  $j$ . So, if  $T \neq \phi$  then  $[v \in \bar{A}(c_i) \text{ and } v \in \bar{A}(c_j), \forall j]$

**R2:** If  $T$  is a vacant set, the data object is being categorized as lower approximation for cluster  $i$ . Then the pixel is categorized as upper approximation for clusters  $i$  as per the hypothesis P2. So, if  $T = \phi$  then  $[v \in \bar{A}(c_i) \text{ and } v \in \underline{A}(c_i)]$

Depending on the above deliberations the algorithm steps for rough k-means are represented as Algorithm 1.

## 3 Experimental Results

The experiment has been performed over 30 plant images using MatlabR2018b on Windows-10 OS, x64-based PC, Intel core i5 CPU with 8 GB RAM. The plant images are collected from [17]. The parameter settings of the utilized clustering techniques are as follows. Number of cluster prototype value depends on the user which is taken as 2 for all clustering techniques. For FCM, fuzzification parameter is taken as 2 and if maximum difference between two successive partition matrices  $U$  is less than minimal error threshold  $\eta$  then stop the corresponding algorithm. Mathematically, if  $[Max U^t - U^{(t+1)}] < \eta$  then stop, where, minimal error threshold  $\eta = 10^{-5}$ . For KM and RKM, if the change in centroid values are smaller

- 1 For each cluster and data object, find the distance  $d$  and threshold  $T$
- 2 Classify the data object to lower and upper estimates utilizing the classification criteria i.e.,  $R1$  and  $R2$ .
- 3 Calculate the new cluster center ( $mean\ z_i$ ) as per following expressions:
- 4 If  $[\underline{A}(c_i) \neq \phi \text{ and } \bar{A}(c_i) - \underline{A}(c_i) = \phi]$
- 5 then  $z_i = \frac{\sum_{v \in A(c_i)} v}{|\underline{A}(c_i)|}$
- 6 else if  $[\underline{A}(c_i) \neq \phi \text{ and } \bar{A}(c_i) - \underline{A}(c_i) \neq \phi]$
- 7 then  $z_i = \frac{\sum_{v \in A(c_i) - \underline{A}(c_i)} v}{|\underline{A}(c_i) - \bar{A}(c_i)|}$
- 8 else  $z_i = w_l \times \frac{\sum_{v \in A(c_i)} v}{|\underline{A}(c_i)|} + w_u \times \frac{\sum_{v \in A(c_i) - \underline{A}(c_i)} v}{|\underline{A}(c_i) - \bar{A}(c_i)|}$
- 9  $w_l + w_u = 1$  and usually,  $w_l > w_u$ . The parameters  $w_l$  and  $w_u$  correspond to the relative importance of lower and upper approximations respectively.
- 10 If the algorithm converges, then stop. Otherwise, repeat steps 2 to 4.

**Algorithm 1:** Procedure of Rough K-Means (RKM)

than  $\eta$  the stop the procedure. The rough set parameters for classical RKM are  $th = 0.7$ ,  $w_l = 0.6$ , and  $w_u = 0.4$ . Threshold ( $th$ ) selection in RKM is tough for different image. We have done the experiment within the range  $0 < th \leq 10$  and optimally set to 0.7. The performance of the utilized clustering techniques has been evaluated by calculating four ground truth based performance evaluation parameters namely accuracy, dice, Jaccard, and Matthews correlation coefficient (MCC) which are summarized in Table 1 [6] [26]. Here, TP - true positive, FP - false positive, TN - true negative, FN - false negative.

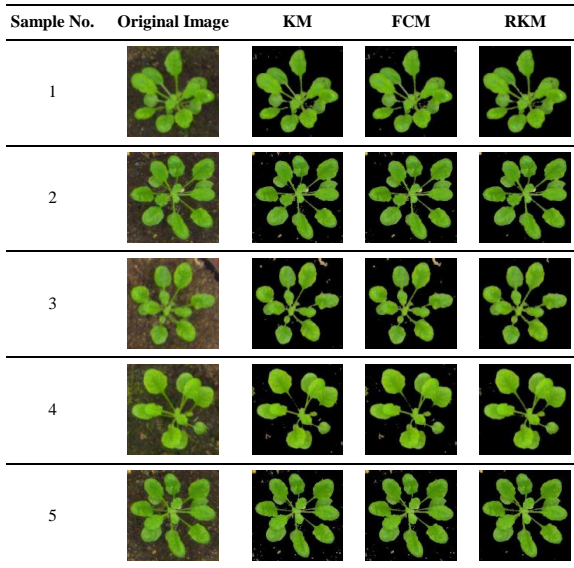


**Figure 2:** Color segmentation results of clustering techniques over five sample images

**Table 1:** Performance parameters considered for evaluation of the clustering methods.

| Sl. | Parameters                             | Formulation and Remarks   |
|-----|--|---|
| 1   | Accuracy (AC)                          | $AC = \frac{(TP+TN)}{(FN+FP+TP+TN)}$ ; Accuracy is one metric for evaluating classification models. We calculate the accuracy to know how good our model predicts.  |
| 2   | Dice Index (DI)                        | $DI = \frac{2 \times \text{Intersection}}{(2 \times TP + FP + FN)}$ ; It combines the precision and recall concepts from information retrieval. It is the harmonic mean of the precision and recall. The DI values are within the interval $[0, 1]$ and larger the value indicates higher clustering quality.   |
| 3   | Jaccard Index (JI)                     | $JI = DI / (2 - DI)$ ; Jaccard similarity index measures the overlap between two sets. It is defined as the size of the intersection of two sets divided by the size of their union. The higher value indicates more similarities between two objects.  |
| 4   | Matthews correlation coefficient (MCC) | $MCC = \frac{(TP \times TN - FP \times FN)}{\sqrt{(TP+FP) \times (TP+FN) \times (TN+FP) \times (TN+FN)}}$ ; (MCC) is a more reliable statistical rate which produces a high score only if the prediction obtained good results in all TP, TN, FP, FN categories and proportionally both to the size of positive elements and the size of negative elements in the dataset. Higher value indicates the better results. |

**Table 2:** Numerical values of segmentation quality parameters over five sample images

| Sample No. | Method     | Accuracy      | Dice          | Jaccard       | MCC           |
|------------|------------|---------------|---------------|---------------|---------------|
| 1          | KM         | 0.9756        | 0.9651        | 0.9325        | 0.9463        |
|            | FCM        | 0.9743        | 0.9633        | 0.9292        | 0.9435        |
|            | <b>RKM</b> | <b>0.9851</b> | <b>0.9791</b> | <b>0.9590</b> | <b>0.9677</b> |
| 2          | KM         | 0.9786        | 0.9720        | 0.9455        | 0.9548        |
|            | FCM        | 0.9819        | 0.9762        | 0.9536        | 0.9617        |
|            | <b>RKM</b> | <b>0.9845</b> | <b>0.9798</b> | <b>0.9603</b> | <b>0.9675</b> |
| 3          | KM         | 0.9730        | 0.9555        | 0.9147        | 0.9364        |
|            | FCM        | 0.9761        | 0.9607        | 0.9244        | 0.9440        |
|            | <b>RKM</b> | <b>0.9773</b> | <b>0.9630</b> | <b>0.9287</b> | <b>0.9476</b> |
| 4          | KM         | 0.9714        | 0.9541        | 0.9122        | 0.9336        |
|            | FCM        | 0.9720        | 0.9552        | 0.9143        | 0.9350        |
|            | <b>RKM</b> | <b>0.9880</b> | <b>0.9810</b> | <b>0.9627</b> | <b>0.9723</b> |
| 5          | KM         | 0.9738        | 0.9659        | 0.9341        | 0.9453        |
|            | FCM        | 0.9793        | 0.9729        | 0.9473        | 0.9565        |
|            | <b>RKM</b> | <b>0.9838</b> | <b>0.9788</b> | <b>0.9585</b> | <b>0.9661</b> |

**Table 3:** Average numerical values of segmentation quality parameters and execution time

| Method     | Accuracy      | Dice          | Jaccard       | MCC           | Time (Sec.) |
|------------|---------------|---------------|---------------|---------------|-------------|
| KM         | 0.9638        | 0.9470        | 0.9001        | 0.9200        | <b>3.78</b> |
| FCM        | 0.9593        | 0.9417        | 0.8909        | 0.9112        | 4.56        |
| <b>RKM</b> | <b>0.9662</b> | <b>0.9531</b> | <b>0.9124</b> | <b>0.9293</b> | 8.26        |

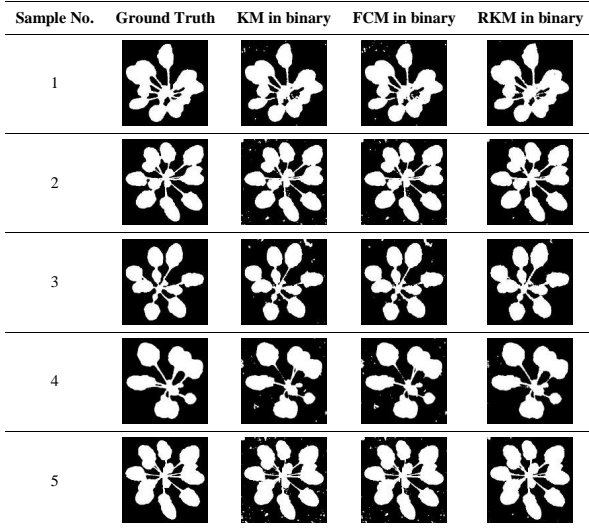


**Figure 3:** Ground truth images and segmentation results of clustering techniques in binary format over five sample images

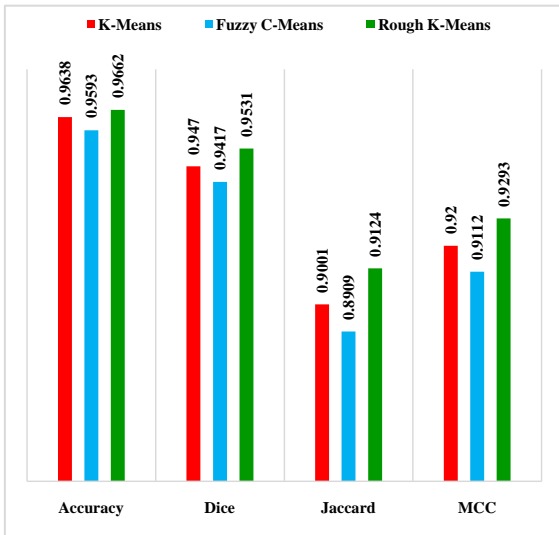


**Figure 4:** Graphical analysis of average quality parameters for clustering techniques

The three clustering algorithms i.e., KM, FCM, and

RKM have been utilized to segment the leaves of the rosette plants. Figure 2 and 3 represents the original color plant image, the ground truth images of the leaf segmentation provided by the experts, their segmented leaf part by the three utilized algorithms binary segmented leaf part provided by the employed clustering algorithms. Figures 2 and 3 here clearly show that the RKM provides the best leaf-based segmentation results. Not only visual analysis, the segmentation efficacy of the clustering algorithms has been analyzed by computing four well-known segmentation quality parameters which are presented in Table 2. The values of the segmentation quality parameters regarding five plant samples presented in Table 2. The average values of the segmentation quality parameters over 30 images are given in Table 3. The best numerical values of the Tables 2 and 3 are given in bold. Most of the values of the quality parameters clearly reveal that RKM provides superior outcomes to other three tested clustering algorithms. The graphical representation of the average quality parameters (recorded in Table 3) is also showed in Figure 4. The average execution times of the four clustering algorithms over 30 images are also presented in Table 3. KM needs least computational effort. RKM takes the largest execution time in the same environment.

## 4 Conclusion

This paper presents a Rough K-Means (RKM) based clustering algorithm in CIELab color space for leaf image segmentation of rosette plants. The proposed RKM based technique is compared against two well-known conventional clustering algorithms namely K-Means and Fuzzy C-Means. An entire dataset of 30 images have been used for this experiment. Experimental results here reveals that the RKM based clustering algorithm outperforms the others and delivers the best outcomes in both the visual as well as numerical analysis for the utilized segmentation parameters. The main three limitations of the proposed method are noise sensitivity, local optima trapping and large computational time. If researched further, it can be possible to analyze the plant's growth or to detect any visually identifiable signs of disease or damage, or any possible visual anomaly. These results encourage further research in the improvement of RKM for image segmentation such as incorporation of nature-inspired optimization algorithms to overcome local optima trapping problem [8] [4].

## References

- [1] AICH, S., AND STAVNESS, I. Leaf counting with deep convolutional and deconvolutional networks. In *Proceedings of the IEEE International Conference on Computer Vision Workshops* (2017), pp. 2080–2089.
- [2] ARBELAEZ, P., MAIRE, M., FOWLKES, C., AND MALIK, J. Contour detection and hierarchical image segmentation. *IEEE transactions on pattern analysis and machine intelligence* 33, 5 (2010), 898–916.

- [3] BEZDEK, J. C., EHRlich, R., AND FULL, W. Fcm: The fuzzy c-means clustering algorithm. *Computers & geosciences* 10, 2-3 (1984), 191–203.
- [4] DHAL, K. G., DAS, A., GÁLVEZ, J., RAY, S., AND DAS, S. An overview on nature-inspired optimization algorithms and their possible application in image processing domain. *Pattern Recognition and Image Analysis* 30, 4 (2020), 614–631.
- [5] DHAL, K. G., DAS, A., RAY, S., AND DAS, S. A clustering based classification approach based on modified cuckoo search algorithm. *Pattern Recognition and Image Analysis* 29, 3 (2019), 344–359.
- [6] DHAL, K. G., DAS, A., RAY, S., AND GÁLVEZ, J. Randomly attracted rough firefly algorithm for histogram based fuzzy image clustering. *Knowledge-Based Systems* 216 (2021), 106814.
- [7] DHAL, K. G., FISTER JR, I., DAS, A., RAY, S., AND DAS, S. Breast histopathology image clustering using cuckoo search algorithm. In *Proceedings of the 5th student computer science research conference* (2018), pp. 47–54.
- [8] DHAL, K. G., FISTER JR, I., AND DAS, S. Parameterless harmony search for image multi-thresholding. In *4th student computer science research conference (StuCosRec-2017)* (2017), pp. 5–12.
- [9] DHAL, K. G., GÁLVEZ, J., RAY, S., DAS, A., AND DAS, S. Acute lymphoblastic leukemia image segmentation driven by stochastic fractal search. *Multimedia Tools and Applications* (2020), 1–29.
- [10] DOBE, O., SARKAR, A., AND HALDER, A. Rough k-means and morphological operation-based brain tumor extraction. In *Integrated Intelligent Computing, Communication and Security*. Springer, 2019, pp. 661–667.
- [11] GHOSAL, D., DAS, A., AND DHAL, K. G. A comparative study among clustering techniques for leaf segmentation in rosette plants. *Pattern Recognition and Image Analysis* 31, 4 (2021).
- [12] INBARANI H, H., AZAR, A. T., ET AL. Leukemia image segmentation using a hybrid histogram-based soft covering rough k-means clustering algorithm. *Electronics* 9, 1 (2020), 188.
- [13] KOORNNEEF, M., HANHART, C., VAN LOENEN-MARTINET, P., AND BLANKESTIJN DE VRIES, H. The effect of daylength on the transition to flowering in phytochrome-deficient, late-flowering and double mutants of *arabidopsis thaliana*. *Physiologia Plantarum* 95, 2 (1995), 260–266.
- [14] KUMAR, D. M., SATYANARAYANA, D., AND PRASAD, M. G. An improved gabor wavelet transform and rough k-means clustering algorithm for mri brain tumor image segmentation. *Multimedia Tools and Applications* 80, 5 (2021), 6939–6957.
- [15] KUMAR, J. P., AND DOMNIC, S. Rosette plant segmentation with leaf count using orthogonal transform and deep convolutional neural network. *Machine Vision and Applications* 31, 1 (2020), 1–14.
- [16] LINGRAS, P., AND WEST, C. Interval set clustering of web users with rough k-means. *Journal of Intelligent Information Systems* 23, 1 (2004), 5–16.
- [17] MINERVINI, M., FISCHBACH, A., SCHARR, H., AND TSAFTARIS, S. A. Finely-grained annotated datasets for image-based plant phenotyping. *Pattern recognition letters* 81 (2016), 80–89.
- [18] NING, J., ZHANG, L., ZHANG, D., AND WU, C. Interactive image segmentation by maximal similarity based region merging. *Pattern Recognition* 43, 2 (2010), 445–456.
- [19] ORLANDO, F., NAPOLI, M., DALLA MARTA, A., NATALI, F., MANCINI, M., ZANCHI, C., AND ORLANDINI, S. Growth and development responses of tobacco (*nicotiana tabacum* l.) to changes in physical and hydrological soil properties due to minimum tillage.
- [20] PAPE, J.-M., AND KLUKAS, C. 3-d histogram-based segmentation and leaf detection for rosette plants. In *European Conference on Computer Vision* (2014), Springer, pp. 61–74.
- [21] PETERS, G. Some refinements of rough k-means clustering. *Pattern Recognition* 39, 8 (2006), 1481–1491.
- [22] RAJ, A., AND MINZ, S. Spatial rough k-means algorithm for unsupervised multi-spectral classification. In *International Conference on Information and Communication Technology for Intelligent Systems* (2020), Springer, pp. 215–226.
- [23] SARKAR, S., DAS, S., AND CHAUDHURI, S. S. A multilevel color image thresholding scheme based on minimum cross entropy and differential evolution. *Pattern Recognition Letters* 54 (2015), 27–35.
- [24] SCHARR, H., MINERVINI, M., FRENCH, A. P., KLUKAS, C., KRAMER, D. M., LIU, X., LUENGO, I., PAPE, J.-M., POLDER, G., VUKADINOVIC, D., ET AL. Leaf segmentation in plant phenotyping: a collation study. *Machine vision and applications* 27, 4 (2016), 585–606.
- [25] TELFER, A., BOLLMAN, K. M., AND POETHIG, R. S. Phase change and the regulation of trichome distribution in *arabidopsis thaliana*. *Development* 124, 3 (1997), 645–654.
- [26] THANH, D. N., PRASATH, V. S., HIEN, N. N., ET AL. Melanoma skin cancer detection method based on adaptive principal curvature, colour normalisation and feature extraction with the abcd rule. *Journal of digital imaging* (2019), 1–12.
- [27] VUKADINOVIC, D., AND POLDER, G. Watershed and supervised classification based fully automated method for separate leaf segmentation. In *The Netherland Congress on Computer Vision* (2015), pp. 1–2.
- [28] WALTER, A., AND SCHURR, U. The modular character of growth in *nicotiana tabacum* plants under steady-state nutrition. *Journal of Experimental Botany* 50, 336 (1999), 1169–1177.

